

EDGE-PRESERVING IMAGE RECONSTRUCTION FOR COHERENT IMAGING APPLICATIONS

Müjdat Çetin[†], William C. Kar[‡], and Alan S. Willsky[†]

[†]Laboratory for Information and Decision Systems, Massachusetts Institute of Technology
77 Massachusetts Ave., Cambridge, MA 02139, USA

[‡] Multi-Dimensional Signal Processing Laboratory, Boston University,
8 Saint Mary's St., Boston, MA 02215, USA

ABSTRACT

We propose a method for edge-preserving regularized reconstruction in coherent imaging systems. In our framework, image formation from measured data is achieved through the minimization of a cost function, which includes non-quadratic regularizing constraints for suppressing noise artifacts, while preserving the object boundaries in the reconstruction. The cost function we use effectively deals with the complex-valued and random-phase nature of the scattered field, which is inherent in many coherent systems. We solve the challenging optimization problems posed in our framework by a novel extension of half-quadratic regularization methods. We present experimental results from three coherent imaging applications: digital holography, synthetic aperture radar, and medical ultrasound. The proposed technique produces images where coherent speckle artifacts are effectively suppressed, and boundaries between different regions in the scene are preserved.

1. INTRODUCTION

This paper addresses image reconstruction problems in coherent imaging. Coherent imaging is based on recording spatial and/or temporal variations in *both* the intensity of a scattered field and its phase. Many microwave, optical, and acoustic sensing applications use coherent imaging, and particular modalities include synthetic aperture radar (SAR), holography, laser imaging, sonar, and medical ultrasound, among others. In both coherent and incoherent imaging tasks, reconstruction of an image from observed data is often an ill-posed inverse problem. Solution of such inverse problems can be achieved through regularization methods, which turn the problem into a well-posed one, and prevent the amplification of measurement noise during the reconstruction process. However, one limitation of straightforward regularization methods, such as Tikhonov regularization, is the suppression of important features in the resulting imagery, such as edges. Recently this issue

This work was supported by the Army Research Office under Grants DAAD19-00-1-0466 and DAAG55-97-1-0013, the Office of Naval Research under Grant N00014-00-1-0089, the Air Force Office of Scientific Research under Grant F49620-96-1-0028, and the National Institutes of Health under Grant NINDS 1 R01 NS34189.

has been successfully addressed by edge-preserving regularization techniques in incoherent imaging applications, such as restoration of blurred and noisy optical images [1], and reconstruction in X-ray tomography [2].

Coherent image reconstruction poses additional challenges that do not appear in incoherent imaging. First, the signals involved are in general complex-valued. Furthermore, in many problems, including SAR and holography of diffuse objects, the phase of the scattered field is a highly random quantity.¹ This leads to two complications. First, due to constructive and destructive interference of scatterers within a resolution cell, conventional coherent images suffer from speckle artifacts.² Second, due to complex-valued, and random-phase nature of the fields, straightforward application of image reconstruction methods, originally designed for incoherent imaging may not produce accurate reconstructions, as we experimentally demonstrate in Section 5.

To address these challenges, we propose an edge-preserving regularization method specifically for coherent imaging tasks. Our approach involves the minimization of an objective function, which contains ℓ_p -norm-based non-quadratic regularization constraints to impose smoothness on the *magnitudes* of the reconstructed complex-valued field reflectivities. To solve such optimization problems, we provide a formal extension of half-quadratic regularization techniques [4] to complex-valued, random-phase fields. This constitutes the major technical contribution of this work. We demonstrate the performance of the resulting method on examples from a number of coherent imaging applications.

2. OVERVIEW OF THE PROPOSED METHOD

We start from the following assumed discrete model for the coherent observation process:

$$\mathbf{y} = \mathbf{T}\mathbf{f} + \mathbf{w} \quad (1)$$

¹This property is known to enable high-quality reconstructions from limited Fourier-offset data in coherent imaging [3]. For this reason, Fourier transform holograms are often constructed using a diffuser to impart essentially random phase to each point in the original scene before recording.

²Speckle appears when the surface being imaged has roughness at the scale of the illuminating wavelength.

where \mathbf{y} denotes the data measured by the sensor and possibly pre-processed (e.g. demodulated), \mathbf{f} is the unknown sampled image, and \mathbf{w} is additive measurement noise, all column-stacked as vectors. \mathbf{T} is a matrix that models the relationship between the underlying field and the measured data. For example, \mathbf{T} may be a band-limited, possibly frequency-offset Fourier transform operator, where the physics of the problem, sensor parameters, and the observation geometry determine the exact structure. Another example for \mathbf{T} , used in tomographic imaging modalities is projection-type operators, such as the Radon transform. In some applications, e.g. in inverse scattering, the observation process cannot be accurately modeled by a linear relationship, as in (1). While we address only the linear case in this paper, the ideas we present are potentially useful in non-linear problems as well, and the method can be generalized to such cases.

Given the observation model in (1), the objective is to obtain a reconstruction of \mathbf{f} , based on the data \mathbf{y} . Conventional image formation techniques vary depending on the particular modality, and include algorithms based on filtered backprojection and inverse Fourier transformation, among others.

In our approach, we find the reconstructed image $\hat{\mathbf{f}}$ as the minimizer of the following cost function:

$$J_0(\mathbf{f}) = \|\mathbf{y} - \mathbf{T}\mathbf{f}\|_2^2 + \lambda \|\mathbf{D}\mathbf{f}\|_p^p \quad (2)$$

where $\|\cdot\|_p$ denotes the ℓ_p -norm, \mathbf{D} is a discrete approximation to the 2-D spatial derivative operator (gradient), $|\mathbf{f}|$ denotes the vector of magnitudes of the complex-valued vector \mathbf{f} , and λ , $p < 2$ are scalar parameters. The first term in (2) is a data fidelity term, while the second term is a regularizing smoothness constraint, reflecting the prior knowledge we impose about the field. Note that the formulation of (2) starts from the observed sensor data \mathbf{y} , and is not simply a post-processing of a formed image.

In order to avoid problems due to non-differentiability of the ℓ_p -norm around the origin when $p \leq 1$, we use a smooth approximation to the ℓ_p -norm in (2) [1]. This leads to the following slightly modified cost function to be used in practice for numerical purposes:

$$J(\mathbf{f}) = \|\mathbf{y} - \mathbf{T}\mathbf{f}\|_2^2 + \lambda \sum_{i=1}^M (|\mathbf{D}\mathbf{f}|_i|^2 + \epsilon)^{p/2} \quad (3)$$

where $\epsilon \geq 0$ is a small constant, $(\cdot)_i$ denotes the i -th element of a vector, and M is the length of the vector $\mathbf{D}\mathbf{f}$. Note that $J(\mathbf{f}) \rightarrow J_0(\mathbf{f})$ as $\epsilon \rightarrow 0$.

Non-quadratic regularizing constraints such as ℓ_p -norms have previously been shown to produce edge-preserving solutions in problems such as image restoration [1] and X-ray tomography [2], where the signals involved are real-valued. In contrast, we are interested in coherent systems such as SAR and holography, where the processed signals are complex-valued. In many cases of interest, the phase of the unknown complex-valued field \mathbf{f} is highly random, and uncorrelated with the phase at neighboring pixels. Based on this observation, regularizing smoothness constraints in such coherent imaging problems should be applied explicitly

to the *magnitudes* $|\mathbf{f}|$ of the complex-valued reflectivities \mathbf{f} . In our framework, this is achieved through the term $\mathbf{D}|\mathbf{f}|$ in (3). This non-linearity in \mathbf{f} makes the optimization problem more challenging than those arising in incoherent imaging applications. In the next section, we propose a novel extension of half-quadratic regularization methods [4] to complex-valued, random-phase fields for achieving efficient and robust numerical solution of the optimization problems of the form (3), posed in our framework.

3. HALF-QUADRATIC REGULARIZATION FOR COHERENT IMAGING

The main idea in half-quadratic regularization is to introduce and optimize a new cost function, which has the same minimum as the original non-quadratic cost function, but one which can be manipulated with linear algebraic methods. In incoherent imaging applications, such a new cost function is obtained by augmenting the original cost function with an *auxiliary* vector.

Currently available half-quadratic regularization methods designed for incoherent imaging cannot handle the more complicated structure of the optimization problems involved in coherent imaging. In order to deal with such complications, we propose using two auxiliary vectors, \mathbf{b} and \mathbf{s} , matched to the structure of the problem, to form an augmented cost function $K(\mathbf{f}, \mathbf{b}, \mathbf{s})$ which satisfies:

$$\inf_{\mathbf{b}, \mathbf{s}} K(\mathbf{f}, \mathbf{b}, \mathbf{s}) = J(\mathbf{f}). \quad (4)$$

In particular, we construct $K(\mathbf{f}, \mathbf{b}, \mathbf{s})$ in such a way that it is quadratic in \mathbf{f} (hence the name half-quadratic) and easy to minimize in \mathbf{b} and \mathbf{s} . Then the minimization of $K(\mathbf{f}, \mathbf{b}, \mathbf{s})$ can be performed through a block coordinate descent approach.

Now, let us consider our particular cost function $J(\mathbf{f})$ of (3). We can show that the following augmented cost function $K(\mathbf{f}, \mathbf{b}, \mathbf{s})$ satisfies the relationship (4) for this $J(\mathbf{f})$ [5]:

$$K(\mathbf{f}, \mathbf{b}, \mathbf{s}) = \|\mathbf{y} - \mathbf{T}\mathbf{f}\|_2^2 + \lambda \sum_{i=1}^M \left[\mathbf{b}_i (|\mathbf{D}\mathbf{S}\mathbf{f}|_i|^2 + \epsilon) + \left(\frac{p}{2\mathbf{b}_i} \right)^{\frac{p}{2-p}} \left(1 - \frac{p}{2} \right) \right] \quad (5)$$

where

$$\mathbf{S} = \text{diag}\{\exp(-j\mathbf{s}_l)\}, \quad (6)$$

with \mathbf{s}_l being the l -th element of the vector \mathbf{s} , and $\text{diag}\{\cdot\}$ denoting a diagonal matrix whose l -th diagonal element is given by the expression inside the brackets. Due to (4), $J(\mathbf{f})$ and $K(\mathbf{f}, \mathbf{b}, \mathbf{s})$ share the same minima in \mathbf{f} . Note that $K(\mathbf{f}, \mathbf{b}, \mathbf{s})$ is a quadratic function with respect to \mathbf{f} .³ We benefit from the half-quadratic structure through the use of

³We have obviously omitted the recipe for finding a valid $K(\mathbf{f}, \mathbf{b}, \mathbf{s})$ from $J(\mathbf{f})$ here. We just want to point out that, given any edge-preserving cost function $J(\mathbf{f})$, the augmented cost function can be found by using convex duality relationships, and we refer the interested reader to [4].

an iterative block coordinate descent method on $K(\mathbf{f}, \mathbf{b}, \mathbf{s})$, in order to find the field $\hat{\mathbf{f}}$ that also minimizes $J(\mathbf{f})$:

$$\hat{\mathbf{s}}^{(n+1)} = \arg \min_{\mathbf{s}} K(\hat{\mathbf{f}}^{(n)}, \hat{\mathbf{b}}^{(n)}, \mathbf{s}) \quad (7)$$

$$\hat{\mathbf{b}}^{(n+1)} = \arg \min_{\mathbf{b}} K(\hat{\mathbf{f}}^{(n)}, \mathbf{b}, \hat{\mathbf{s}}^{(n+1)}) \quad (8)$$

$$\hat{\mathbf{f}}^{(n+1)} = \arg \min_{\mathbf{f}} K(\mathbf{f}, \hat{\mathbf{b}}^{(n+1)}, \hat{\mathbf{s}}^{(n+1)}) \quad (9)$$

where n denotes the iteration number. Using results from [5], we obtain:

$$\hat{s}_i^{(n+1)} = \phi[(\hat{\mathbf{f}}^{(n)})_i] \quad (10)$$

$$\hat{\mathbf{b}}_i^{(n+1)} = \frac{p}{2 \left[(\mathbf{D}\hat{\mathbf{S}}^{(n+1)}\hat{\mathbf{f}}^{(n)})_i^2 + \epsilon \right]^{1-p/2}} \quad (11)$$

$$\begin{aligned} & \left[\mathbf{T}^H \mathbf{T} + \lambda (\hat{\mathbf{S}}^{(n+1)})^H \mathbf{D}^T \text{diag} \left\{ \hat{\mathbf{b}}_i^{(n+1)} \right\} \mathbf{D} \hat{\mathbf{S}}^{(n+1)} \right] \hat{\mathbf{f}}^{(n+1)} \\ & = \mathbf{T}^H \mathbf{y} \end{aligned} \quad (12)$$

where $\phi[z]$ denotes the phase of the complex number z . We can substitute (10) and (11) into (12) to obtain a single iterative expression for $\hat{\mathbf{f}}^{(n+1)}$, which would then constitute the overall iterative algorithm. Note that each iteration in (12) requires the solution of a set of linear equations for the unknown $\hat{\mathbf{f}}^{(n+1)}$. We use the conjugate gradient algorithm for this solution. We run the iteration (12) until $\|\hat{\mathbf{f}}^{(n+1)} - \hat{\mathbf{f}}^{(n)}\|_2^2 / \|\hat{\mathbf{f}}^{(n)}\|_2^2 < \delta$, where $\delta > 0$ is a small constant. Convergence properties of algorithms of this type have been analyzed, and convergence from any initialization to a local minimum is guaranteed [2, 6].

4. EXTENSIONS

We mention two extensions we have developed [5]. First, some applications may require preservation of features other than, or in addition to edges. We have demonstrated such an extension of our framework for the particular application of SAR imaging, where we have incorporated additional regularizing constraints whose role is to localize and superresolve scatterers with spatially concentrated energy. Second, we have extended our formulation and iterative algorithm to Mumford-Shah-type [7] variational formulations. This extension enables the use of Mumford-Shah-type cost functions in problems involving complex-valued, random-phase fields, and non-trivial observation models.

As another simple extension, note that the use of non-quadratic potential functions other than ℓ_p -norms in $J(\mathbf{f})$ simply requires finding and using the augmented cost function that corresponds to the particular potential function used, without affecting the general coordinate-descent-based algorithmic strategy.

5. EXPERIMENTAL RESULTS

We demonstrate our technique on three imaging applications: digital holography, SAR, and medical ultrasound.

We choose the hyperparameters that appear in the cost function $J(\mathbf{f})$ of (3) based on subjective qualitative assessment.

Figure 1 contains the results of the holography experiment. We multiply the intensity of the original scene in Figure 1(a) at each pixel with a uniformly distributed random phase factor (uncorrelated from pixel to pixel), and compute a band-limited Fourier hologram. The image in Figure 1(b) is the magnitude of the conventional reconstruction from the hologram. This result is dominated by coherent speckle artifacts. The reconstruction produced by our technique ($p = 1.2$) is shown in Figure 1(c). With suppressed speckle, and preserved edges, our method provides a much more accurate reconstruction of the original scene. We next show why some related, but simpler techniques would fail in this problem. In Figure 1(d), we show the result of an incoherent edge-preserving reconstruction method. Since such techniques have been designed for real-valued signals, they are not able to treat the magnitude and phase components properly. This leads to some smoothing effect in the real and imaginary components of the field, however a speckle-dominated magnitude image is produced which shows only minor improvement over the conventional image of Figure 1(b). In Figure 1(e) we present the result of applying edge-preserving regularization (anisotropic diffusion) on the magnitude of the conventionally reconstructed image. Some speckle suppression seems to have been achieved, however significant amount of detail in the scene has been lost. This shows the power of our model-based reconstruction technique in contrast to a post-processing approach for image enhancement.

For the remaining examples in this section, we present just images produced by the conventional and the proposed methods. An additional analysis similar to that carried out for the digital holography example of Figure 1 yields qualitatively very similar results.

Figure 2(a) contains a conventional SAR image of three vehicles in a field containing some trees. Speckle artifacts, clearly visible in this reconstruction, make e.g. automatic segmentation of SAR images very challenging. In contrast, the image produced by our method ($p = 0.7$) produces regions (vehicle, tree, shadow, background) which appear to be more easily separable.

Our final example is from medical ultrasound imaging. A conventional image, shown in Figure 3(a), exhibits speckle artifacts. Our technique ($p = 0.7$) produces the image in Figure 3(b), where such artifacts are reduced, and tissue boundaries appear to have been preserved. Evaluating the medical significance of such reconstructions is a subject currently on our agenda.

6. CONCLUSIONS

We have developed a new approach for image formation in coherent systems. Our method poses the problem as the optimization of a cost function in a regularized data inversion framework. Here, we incorporate edge-preserving potential functions that take into account the nature of the signals involved in coherent imaging. The major technical contribution of this work is the extension of half-quadratic regularization methods to efficiently solve such optimization

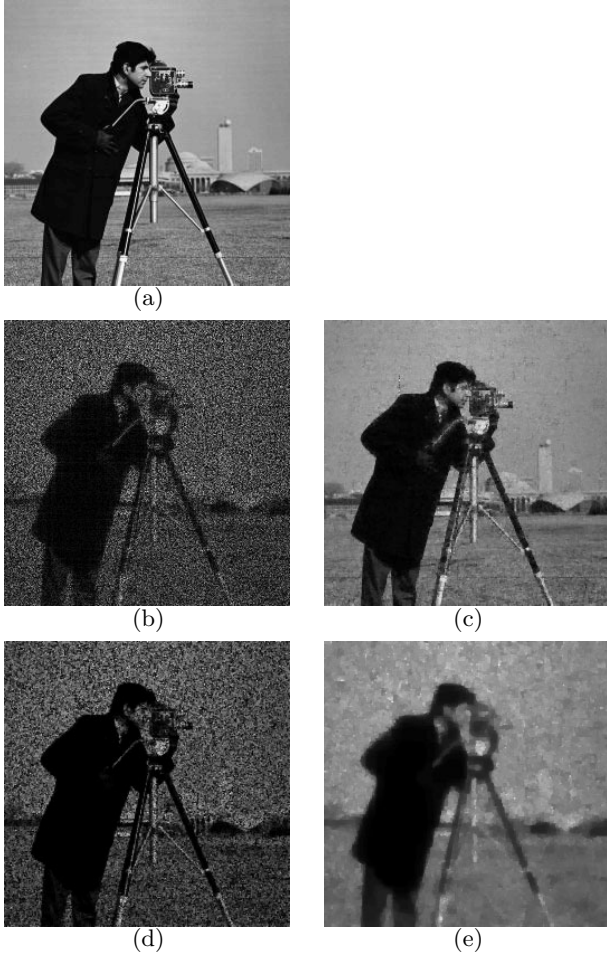


Fig. 1. Reconstruction of an image from its band-limited Fourier hologram. (a) Original scene. (b) Conventional reconstruction. (c) Proposed method with $p = 1.2$. (d) Reconstruction by an edge-preserving regularization method designed for incoherent imaging. (e) Post-processing of the conventionally reconstructed image by edge-preserving regularization (anisotropic diffusion).

tion problems formulated for coherent imaging. Our experimental study has shown the effectiveness of this strategy in obtaining reconstructions that are superior in a number of ways to conventional coherent images. The improvements provided by these reconstructions appear to be promising for visual and automatic interpretation of the underlying scenes. Our current work involves application of the technique on a variety of other data sets, and in coherent imaging applications not considered in this paper.

7. ACKNOWLEDGMENTS

We would like to thank Jeffrey H. Shapiro and Raymond C. Chan for discussions about the work in this paper, and Andy Tsai for providing the ultrasound data.

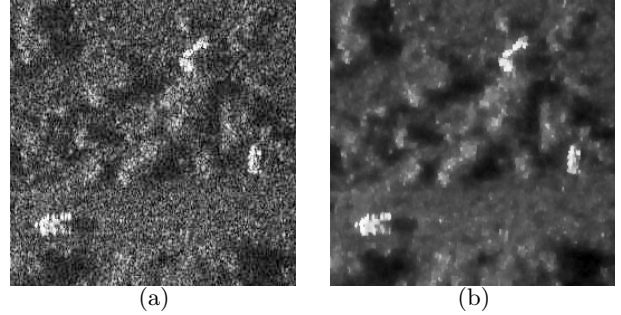


Fig. 2. (a) Conventional SAR image of a scene. (b) Reconstruction produced by the proposed method with $p = 0.7$.

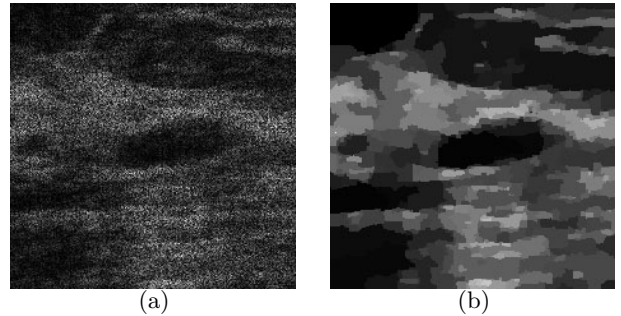


Fig. 3. (a) A conventional ultrasound image. (b) Reconstruction produced by the proposed method with $p = 0.7$.

8. REFERENCES

- [1] C. R. Vogel and M. E. Oman, “Fast, robust total variation-based reconstruction of noisy, blurred images,” *IEEE Trans. Image Processing*, vol. 7, no. 6, pp. 813–824, June 1998.
- [2] P. Charbonnier, L. Blanc-Féraud, G. Aubert, and M. Barlaud, “Deterministic edge-preserving regularization in computed imaging,” *IEEE Trans. Image Processing*, vol. 6, no. 2, pp. 298–310, Feb. 1997.
- [3] D. C. Munson Jr. and J. L. C. Sanz, “Image reconstruction from frequency-offset Fourier data,” *Proc. IEEE*, vol. 72, pp. 661–669, June 1984.
- [4] D. Geman and G. Reynolds, “Constrained restoration and the recovery of discontinuities,” *IEEE Trans. Pattern Anal. Machine Intell.*, vol. 14, no. 3, pp. 367–383, Mar. 1992.
- [5] M. Çetin, *Feature-Enhanced Synthetic Aperture Radar Imaging*, Ph.D. thesis, Boston University, Feb. 2001.
- [6] A. H. Delaney and Y. Bresler, “Globally convergent edge-preserving regularized reconstruction: an application to limited-angle tomography,” *IEEE Trans. Image Processing*, vol. 7, no. 2, pp. 204–221, Feb. 1998.
- [7] D. Mumford and J. Shah, “Boundary detection by minimizing functionals, I,” in *IEEE Conference on Computer Vision and Pattern Recognition*, 1985, pp. 22–26.